International Journal of Mechanical System Dynamics

WILEY

IJMSD International Journal of Mechanical System Dynamics Open Access

RESEARCH ARTICLE OPEN ACCESS

Uncertainty, Sensitivity, and Efficiency Analysis of a Hybrid Piezoelectric–Electromagnetic Energy Harvester

Petr Sosna[1] | Damian Gaska[2] | Zdeněk Hadaš[1]

[1]Faculty of Mechanical Engineering, Brno University of Technology, Brno, Czech Republic | [2]Faculty of Transport and Aviation Engineering, Silesian University of Technology, Katowice, Poland

Correspondence: Petr Sosna (Petr.Sosna@vut.cz)

Received: 17 October 2025 | **Revised:** 16 February 2026 | **Accepted:** 4 March 2026

Funding: European Regional Development Fund, Grant/Award Number: CZ.02.01.01/00/22_008/0004634/Mechanical Engineeri; Grantová Agentura Ceské Republiky, Grant/Award Number: 25-14505L/Advanced techniques for effective kinet

Keywords: electromagnetics | energy harvesting | multidisciplinary model | piezoelectric | sensitivity | uncertainty | vibrations

ABSTRACT

Digitalization and emerging technologies are increasing the demand for wireless sensing and the Internet of Things (IoT), which provide opportunities for autonomous sources of electricity in the form of energy harvesting systems. This paper focuses on the challenges in hybrid piezoelectric-electromagnetic kinetic energy harvesting systems that deliver output power at milliwatt levels, sufficient for current IoT electronics. The main task in the employment of energy harvesting technology for industrial applications is transitioning from laboratory test samples to industrial-scale prototype deployment, with emphasis on sensitivity and uncertainty analyses of energy harvesting parameters. This paper analyses this problem using a single-degree-of-freedom model for a hybrid piezoelectric-electromagnetic kinetic energy harvester, where the effect of uncertainty in design and material input parameters on harvested power outputs is examined. Industrial application uncertainties, including manufacturing and geometric tolerances, uncertainties in material parameters, and fluctuations in ambient input parameters, are assessed and analyzed using the Saltelli method. Key findings highlight the amplification of uncertainties, with mechanical damping identified as the most influential parameter of harvested power. By investigating piezoelectric and electromagnetic coupling factors, this study provides actionable insights for optimizing hybrid energy harvesters and adjusting coupling parameters for maximal output power generation.

1 | Introduction

The growing global industrial digitalization requires sustainable Internet of Things applications, and it accentuates the strong demand for autonomous energy sources, mainly for kinetic energy harvesting systems. Many IoT sensors operate in vibratory environments, and the methods of kinetic energy harvesting principles could provide an autonomous source of energy for IoT sensing applications. The last 20 years have seen an increased focus on the development and integration of energy harvesting (EH) technologies [1–3] for autonomous wireless sensing nodes. These technologies aim to replace or reduce dependence on conventional batteries, which are costly and inefficient to manage at scale [4, 5]. Piezoelectric (PE) [6, 7] and electromagnetic (EM) [8] principles of energy harvesting converters have emerged as effective energy harvesting solutions. Currently, various solutions of kinetic energy harvesters with different design concepts have been proposed, designed, tested, and analyzed, including those with nonlinear or multi-stable characteristics [9], and also excited by impulse [10] or colored noise [11].

Hybrid PE–EM energy harvesters represent an alternative strategy aimed at improving overall performance by combining

two transduction mechanisms within a single device. Many publications deal with the design and development of such hybrid kinetic energy harvesting systems, which could convert vibration energy into useful electricity. Developed hybrid energy harvesting systems integrating both PE and EM technologies show promise for broader operational efficiency and reliability in industrial applications [12–15]. However, recent studies indicate that hybridization does not universally guarantee superior performance. Truong et al. [16] (2023) demonstrated that, depending on excitation conditions and electrical loading, hybrid PE–EM systems may offer limited or no advantage over optimized standalone harvesters. Similarly, Bahadur et al. [17] compared hybrid and standalone harvesters under vortex-induced vibrations and showed that the relative benefit of hybridization strongly depends on coupling strength and damping distribution. These findings highlight that hybridization should be treated as a design option requiring quantitative justification rather than as an inherently superior solution.

From an industrial deployment perspective, performance robustness and repeatability are at least as important as peak power. Consequently, there is a growing need for uncertainty-aware modeling frameworks that quantify performance variability and identify the parameters that most strongly influence system behavior. This work addresses this need by presenting an uncertainty, sensitivity, and efficiency analysis of a hybrid PE–EM energy harvester. The objective is not only to evaluate nominal performance, but also to determine how uncertainties redistribute influence between piezoelectric and electromagnetic subsystems and to assess under which conditions hybridization provides a tangible advantage over standalone harvesting concepts.

2 | State-of-Art—Uncertainty, Sensitivity, and Robustness in Energy Harvesting Systems

In practical applications, energy harvesters are subject to multiple sources of uncertainty that can significantly influence their dynamic and electrical response. These sources include geometric tolerances arising from manufacturing and assembly processes, variability in material properties such as piezoelectric coefficients and magnetic parameters, uncertainty in damping and electrical loading, and variability in excitation amplitude and frequency content. Experimental investigations have shown that even small deviations in these parameters can result in noticeable shifts in resonance frequency and substantial variations in harvested power. Peralta et al. [18] demonstrated that mounting conditions and boundary uncertainties alone can lead to measurable dispersion in frequency response functions, even when measurement noise is negligible. For narrowband harvesters, uncertainty-induced resonance detuning can cause dramatic performance degradation.

To address performance variability, uncertainty quantification (UQ) techniques have been increasingly adopted in the energy harvesting literature [19]. Mann et al. [20] highlighted the importance of uncertainty when comparing linear and nonlinear harvesting strategies, showing that conclusions based on nominal parameters may not hold under realistic variability. Aloui et al. [21] applied probabilistic UQ and global sensitivity analysis to a piezoelectric energy harvester and demonstrated that only a small subset of parameters dominates output variability. In nonlinear and multi-stable harvesters, uncertainty can additionally induce qualitative changes in dynamic response, such as transitions between coexisting attractors [22]. As a result, two harvesters with the same nominal design can exhibit noticeably different frequency response functions and output power.

Global sensitivity analysis, particularly variance-based methods such as Sobol sensitivity indices, has become a key tool for identifying influential parameters and interaction effects. Norenberg et al. [23] showed that interaction effects can play a dominant role in asymmetric nonlinear energy harvesters under uncertainty. Interval-based uncertainty analysis has also been applied to nonlinear and bistable energy harvesters. Li et al. [24] employed an improved interval extension approach to show that bounded parameter uncertainty can significantly alter the predicted response envelopes of bistable harvesters, highlighting the limitations of purely nominal or deterministic analyses in nonlinear regimes.

Beyond analysis, robust design methodologies seek to optimize harvester performance while explicitly accounting for uncertainty. Martins and Santos [25] introduced a Kriging-based metamodeling approach for multi-objective robust optimization of energy harvesting devices, demonstrating improved reliability compared to nominally optimized designs. Collectively, these studies establish that neglecting uncertainty can lead to overly optimistic performance predictions [26], reduced reproducibility across prototypes, and misleading conclusions regarding parameter importance—particularly for harvesters relying on narrow resonance peaks.

While uncertainty and robust design are increasingly studied for **single-mechanism** harvesters (piezoelectric-only, electromagnetic-only, or purely nonlinear benchmark models), **uncertainty-driven analysis focused on hybrid piezoelectric–electromagnetic (PE–EM) harvesters** remains comparatively limited—especially in a form that is (i) **design-oriented** (linked to measurable geometry/material parameters and manufacturing sources) and (ii) interpretable for **industrial deployment** decisions (what to control tightly, what can be relaxed, and when hybridization is actually beneficial).

3 | Motivation—From Laboratory Prototypes to Industrial Deployment

The nominal values in mathematical or simulation model might tell us what power is expected, but they do not show how much it could actually vary in industrial conditions, and this is the main motivation of our research paper. By quantifying the impact of uncertainties and sensitivities of hybrid PE-EM energy harvesting parameters, this work aims to bridge the gap between laboratory-based modeling and reliable industrial deployment.

The main goal of our research is to analyze parameters of PE-EM energy harvesting systems in detail to advance robust and adaptable design of hybrid energy harvesters for wide industrial applications.

Based on the reviewed literature, several research gaps can be identified. First, there is a lack of comprehensive uncertainty-driven analyses specifically targeting hybrid PE–EM energy harvesters. Second, the redistribution of sensitivity between piezoelectric and electromagnetic subsystems under uncertainty

has not been sufficiently investigated. Third, existing studies provide limited guidance on which parameters require tight control to ensure robust performance and which parameters can tolerate variability.

Addressing these gaps is essential for transitioning hybrid energy harvesting concepts from laboratory demonstrations to reliable industrial solutions. This paper focuses on hybrid piezoelectric-electromagnetic energy harvesters designed for industrial use, especially in the aircraft and railway applications of autonomous structural monitoring. However, many of these systems remain confined to laboratory prototypes in TRL level up to 4, and the operation is optimized in controlled environment settings and testing.

To address this gap, the present paper adopts a hierarchical evaluation framework that extends beyond nominal performance analysis. In addition to conventional modeling and simulation, the approach integrates local sensitivity analysis, global uncertainty quantification, and coupling-parameter effectiveness analysis. The proposed development steps are shown in Figure 1.

Through the proposed analysis, critical parameters that require precise control during manufacturing and deployment are identified, while parameters with minimal impact can be recognized, allowing relaxed tolerances and potential cost savings. Sensitivity analysis also guides device tuning by indicating which parameters should be adjusted and in which direction to optimize individual harvesters within a population. This analysis must be complemented by an uncertainty analysis that accounts for unpredictable variations arising from manufacturing tolerances and operational environments, such as fluctuating vibration levels. The final step of the proposed framework (Level V) is required because identifying sensitive parameters and quantifying uncertainty alone does not indicate how individual harvesters within a population should be adjusted. Level V, therefore, transforms the results of sensitivity and uncertainty analyses into practical fine-tuning strategies by indicating which parameters can be adjusted, in which direction, and by how much for individual harvesters to compensate for manufacturing and operational variability. This step enables post-assembly tuning of devices to recover or improve performance rather than relying solely on nominal optimization.

While uncertainty quantification and sensitivity analysis have been extensively studied for energy harvesting systems, the present work does not claim methodological novelty in these techniques. Instead, its main contribution lies in its systematic integration into a hierarchical evaluation framework tailored to hybrid PE–EM energy harvesters and explicitly aimed at supporting industrial deployment decisions.

By providing a comprehensive uncertainty-aware evaluation of hybrid energy harvesting systems, this work aims to support the design of reliable and adaptable devices capable of operating beyond laboratory conditions and enabling autonomous power supply for wireless sensing at an industrial scale.

Furthermore, a design of power management electronics for a multi-source combination is being studied and developed [27]. It is extremely challenging to identify conditions where all individual physical principles of energy harvesting systems can operate efficiently. This challenge also motivates the present study, which focuses on understanding how coupled electro-mechanical subsystems interact under realistic operating conditions.

4 | Mathematical Coupled Model of Hybrid Energy Harvesting System

This section introduces the well-known mathematical framework used throughout the key sensitivity and uncertainty analyses. While the coupled differential equations of motion are widely used in energy harvesting models, the novelty of the present work lies in the comprehensive and systematic application of these models to identify sources of uncertainty, parameter sensitivities, and their implications for industrial

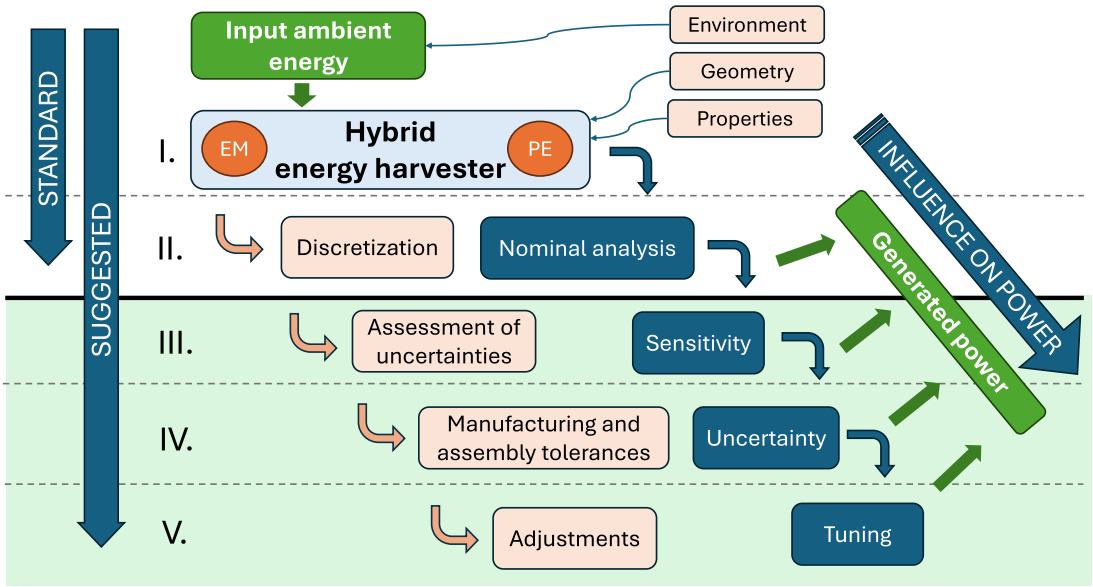

FIGURE 1 | Suggested new approach for the evaluation of the power output of energy harvesters. Levels I and II represent standard practices widely used in current literature, including discretization and nominal performance analysis under idealized conditions. Levels III to V highlight the novel contribution of this paper—integrating sensitivity analysis, uncertainty quantification, and effective parameter tuning.

deployment of hybrid piezoelectric–electromagnetic energy harvesters.

The structure of this chapter is intentionally hierarchical. It starts from a compact, commonly used representation and progresses to formulations in which physical parameters and uncertainty sources become explicit. Initially, it presents a baseline 1-DOF lumped-parameter model that is commonly used to describe hybrid PE–EM harvesters. This formulation serves as a reference model and is subsequently employed in the local sensitivity analysis presented in Section 5. Furthermore, in Sections 4.1 and 4.2, the model is expanded to explicitly express the piezoelectric and electromagnetic subsystems in terms of measurable geometric, material, and physical parameters. This expansion is essential for making individual sources of uncertainty visible and physically interpretable. Finally, Section 4.3 introduces the probabilistic formulation of the model, in which selected parameters are treated as random variables. This uncertain model forms the basis for the global sensitivity and uncertainty analyses presented in Section 6.

4.1 | 1-DOF Model With Discretized Parameters

Piezoelectric layers in the bimorph configuration are attached to the beam resonator under harmonic excitation. The mechanical strain in the piezoelectric layer under deformation produces an electric charge on the piezoelectric electrodes via the direct piezoelectric effect.

The electromagnetic converter consists of a magnetic circuit, the main part of the tip mass, and a coil fixed to the frame. The resonance operation provides a relative movement of the magnetic circuit against the coil, and on the basis of Faraday's Law, an electromotive voltage is induced on the coil. Both PE and EM converters are individually connected to the electrical loads. This analysis expected optimal resistive loads for both converters. However, advanced electronics, including a rectifier and power management, could be used in the target industrial application.

This concept of a hybrid PE-EM energy harvester is shown in Figure 2. There are four subsystems: vibration excitation of mechanical resonator, piezoelectric, and electromagnetic converters. Additionally, a fifth subsystem could be the electrical load as a model of power management electronics.

For the analysis and further optimization of the behavior of the hybrid energy harvesting system, the one degree of freedom (1DOF) mathematical model is presented. The discretization procedure for the piezoelectric composite beam is well understood and described in papers such as [28]. When combined with the model of the electromagnetic converter, described, for example, in [3], the resulting 1DOF has the following form:

$$m\ddot{y} + d_m\dot{y} + ky + C_{\mathrm{EM}}i_e + \theta V_p = \ddot{z}\sin(2\pi ft), \tag{1}$$

$$\theta\dot{y} = \dot{V}_p C_p + \frac{V_p}{R_p}, \tag{2}$$

$$C_{\mathrm{EM}}\dot{y} = L_C\frac{\mathrm{d}i_e}{\mathrm{d}t} + i_e R_C + i_e R_e. \tag{3}$$

The model is described by three coupled electro-mechanical equations, namely the second-order differential equation of mechanical motion for the vibration of the beam (Equation [1]) and two first-order coupled electrical equations for the piezoelectric (Equation [2]) and electromagnetic (Equation [3]) circuits. The coupled 1DOF model of the hybrid harvester has a total of 12 independent parameters. However, such parameters are calculated by modeling individual geometric, material, and physical parameters. The discretized mass m includes material and geometric parameters of the steel beam, piezoelectric layers, and magnetic circuit, linear stiffness k describes beam stiffness, d_m is experimentally identified mechanical damping, C_{EM} is electromechanical coupling [3], θ is piezoelectric coupling, C_p is capacitance of the piezoelectric layer, R_c is resistance of the coil, L_c inductance of the coil and Z_e and Z_p are impedances of connected electric loads to the electromagnetic and piezoelectric converters. In this paper, the impedances are only pure resistive with optimal values R_e and R_p. The system is excited by harmonic vibrations of amplitude $\ddot{z}$ and frequency f. There are three dependent system state variables, deflection of the tip mass of the beam y, voltage on the piezoelectric element V_p and current in the coil i_e. The 1DOF representation of the energy harvesting system is shown in Figure 3.

This simplified coupled model of hybrid vibration energy harvester (Figure 3) is universal in the sense that it can also be used for the description of both systems separately by setting their corresponding coupling coefficients to zero. Throughout the paper, the following color representation of the subsystems is followed:

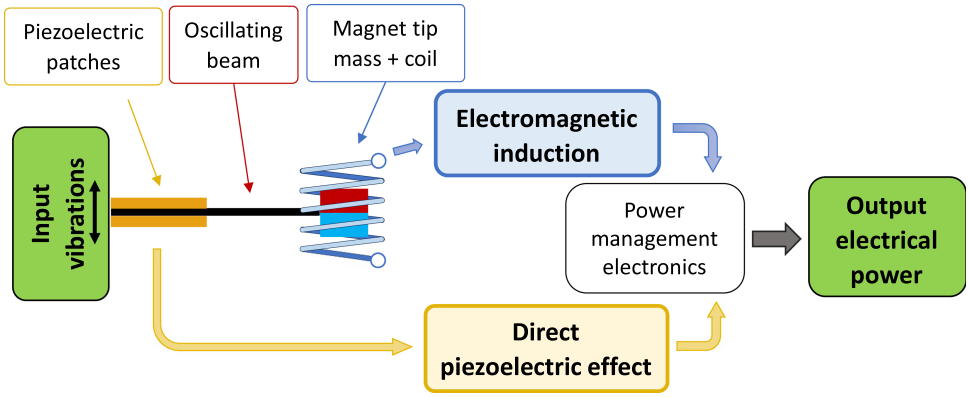

FIGURE 2 | Schematic diagram of the proposed hybrid energy harvesting system with piezoelectric layers and electromagnetic system.

mechanical—red, piezoelectric—orange, electromagnetic—blue, and excitation—green.

4.2 | Expanded Mathematical Model for Piezoelectric Harvester

In this section, the PE transducer is analyzed in detail. The basic 1DOF coupled model (Equations [1]–[3]) is used throughout the entire paper, but here it is expanded to contain more basic and measurable parameters. The expansion is done to a certain extent using analytical expressions developed in Refs. [29] and [28]. By incorporating measurable factors such as geometrical dimensions and material properties, we aim to pave the way for a more nuanced evaluation of the hybrid system performance under diverse conditions.

The piezoelectric model contains MFC industrial piezoelectric patches labeled as MFC2814—P2 from the company Smart Materials in the piezoelectric 31 operation mode. These patches emerged in the last decade [30] and now seem to be getting more popular thanks to their convenience in various fields [31]. The MFC patches are a composite material consisting mainly of PZT fibers in an epoxy matrix. Copper electrodes are on top and bottom, and these two components are covered in polyimide film. A numerical homogenization procedure was developed in Ref. [32], which calculates the orthotropic elastic and piezoelectric properties of the MFC.

The PE coupling coefficient is further expanded to show how some of the input parameters, such as the dimensions of the piezoelectric layer, or the material, affect the generated power. The piezoelectric coupling coefficient θ can therefore be calculated as

$$\theta = -\int_{V_p} y \frac{\partial^2 \phi(x)}{\partial x^2} e_{31} \psi(z) \mathrm{d}V_p \tag{4}$$

As is shown in Figure 4, the dimensions of the layers are $V_p = t_p \times L_p \times B_p$ and of the steel substrate $V_s = t_s \times L_s \times B_s$. The beam is to be excited with frequencies around its first natural frequency; therefore, the first bending mode shape $\phi(x)$ is dominant. Because the PE element is shorter than the substrate, the beam is not uniform along its length. Analytical equations could be used to describe this function, but here we decided to use FEM modal analysis in the Ansys Workbench environment. We note that the piezoelectric behavior is not assumed for the purpose of mode shape, so the mode shape is affected only by the variable stiffness.

The piezoelectric stress-charge constant e_{31} is related to the strain charge constant d_{31} by multiplying an element of the compliance matrix s_{11} such that $e_{31} = d_{31} s_{11}$. The d_{31} constant is calculated using the homogenization procedure of the MFC.

Equation (4) can now be manipulated further and integrated. The integration is through the volume of the PE element; therefore, according to Figure 4, the interval in the y direction is from t_s to $\frac{t_s}{2} + t_p$ for the upper element and similarly for the lower one with negative signs. Further modification and simplification lead to the following algebraic equation for the PE coupling coefficient.

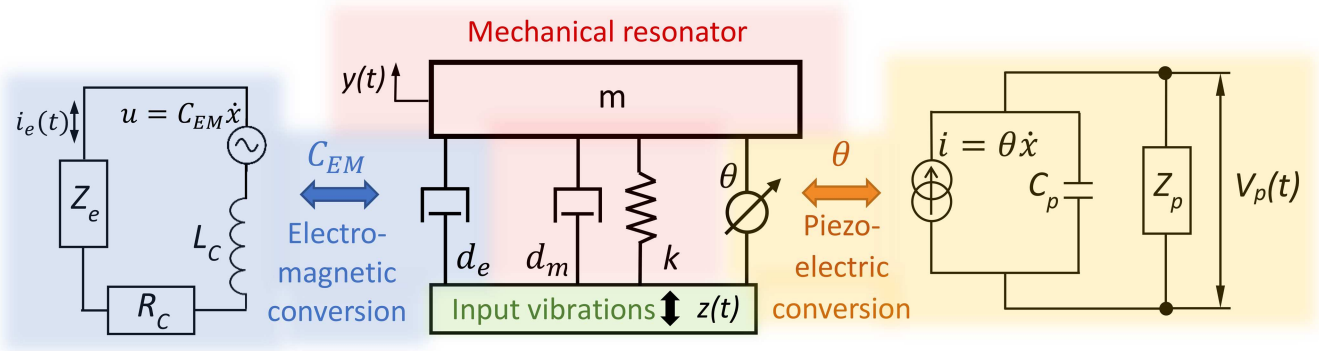

FIGURE 3 | 1DOF model of the energy harvesting system with coupled subsystems. Piezoelectric coupling is characterized by θ, electromagnetic coupling by C_{EM}.

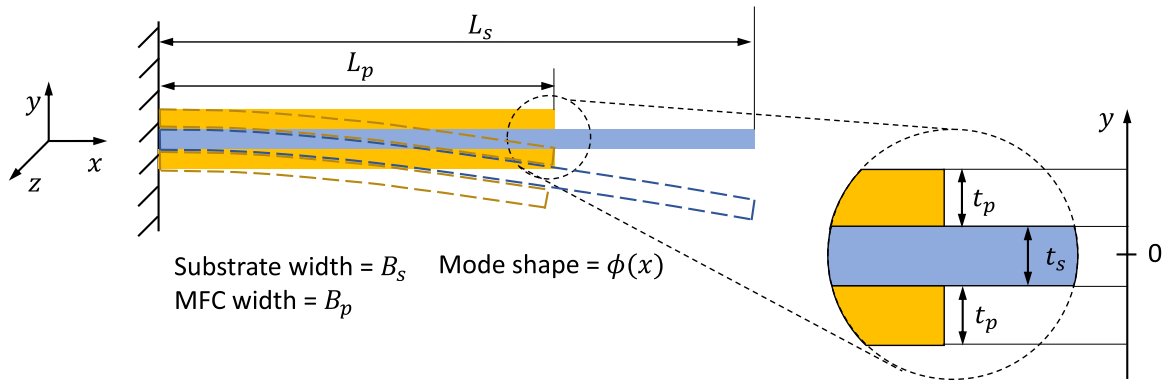

FIGURE 4 | Schematic of the composite beam consisting of steel substrate and piezoelectric MFC layers.

$$\theta = \frac{-B_p \frac{d_{31}}{s_{11}}(t_p + t_s)\frac{\partial \phi}{\partial x}(L_p)}{\phi(L_s)} = -B_p e_{31}(t_p + t_s)\gamma, \tag{5}$$

$$\gamma = \frac{\partial \phi}{\partial x}(L_p)/\phi(L_s), \tag{6}$$

where $\gamma = \frac{\partial \phi}{\partial x}(L_p)/\phi(L_s)$ is a scalar that describes the mode shape. The MFC layers are assumed to act as linear capacitors with a constant electric field E inside, therefore,

$$E = \psi(z)V(t) = \begin{cases} -\frac{V}{t_p} & \frac{t_s}{2} < y < \frac{t_s}{2} + t_p \quad \text{(upper element)} \\ \frac{V}{t_p} & -\frac{t_s}{2} - t_p < y < -\frac{t_s}{2} \text{ (lower element)}, \end{cases} \tag{7}$$

where $\psi(z)$ is the electric field distribution function. The mentioned Ref. [29] also provides an equation for the capacitance C_p,

$$C_p = \int_{V_p} \varepsilon_{33} \psi^2(z) \mathrm{d}V_p = 2\varepsilon_{33} \frac{B_p L_p}{t_p}, \tag{8}$$

where ε_{33} is an element of the permittivity matrix of the PE component.

4.3 | Model of Electromagnetic Harvester

The core principle that governs electromagnetic vibration energy harvesters is Faraday's law of electromagnetic induction. The induced voltage V_e in a coil with N turns and an active length l which moves with a velocity $\dot{y}$ in a magnetic flux density field B is calculated as the time derivative of the changing magnetic flux Φ.

$$V_e = \frac{\mathrm{d}\Phi}{\mathrm{d}t} = BNl\dot{y}. \tag{9}$$

The electromechanical coupling is defined as

$$C_{\mathrm{EM}} = NBl, \tag{10}$$

where Nl is the total active length of the coil, and the total resistance of coil is R_C.

The induced voltage causes current flow i_e through a connected resistive load R_e, which creates additional damping feedback—an electromagnetic damping force F_d [33]

$$F_d = d_e \dot{y} = \frac{(NBl)^2 \dot{y}}{R_e + R_C}. \tag{11}$$

4.4 | Model of Input Uncertainties of Coupled Hybrid Kinetic Energy Harvester

Since all the input parameters can now have individual input uncertainties, the parameters can be thought of as probabilistic parameters, and each is described by its probability density function. If all the distributions were normal and characterized by mean value μ and standard deviation σ, then the coupled equations could be written with probabilistic variables in capital letters as

$$m\ddot{y} + D_m(\mu_{d_m}, \sigma_{d_m})\dot{y} + ky + C_{EM}(\mu_{C_{EM}}, \sigma_{C_{EM}})i_e + \theta(\mu_\theta, \sigma_\theta)V_p = \ddot{Z}(\mu_{\ddot{z}}, \sigma_{\ddot{z}})\sin(2\pi F(\mu_F, \sigma_F)t), \tag{12}$$

$$\theta(\mu_\theta, \sigma_\theta)\dot{y} = \dot{V}_p C_p(\mu_{C_p}, \sigma_{C_p}) + \frac{V_p}{R_p(\mu_{R_p}, \sigma_{R_p})}, \tag{13}$$

$$C_{EM}(\mu_{C_{EM}}, \sigma_{C_{EM}})\dot{y} = i_e R_C(\mu_{R_C}, \sigma_{R_C}) + i_e R_e(\mu_{R_e}, \sigma_{R_e}) + L_C(\mu_{L_C}, \sigma_{L_C})\frac{\mathrm{d}i_e}{\mathrm{d}t}, \tag{14}$$

Equations (12)–(14) now form the basis for the analysis described in the next section.

In this work, we only consider the simplest model of energy harvesting, which is done through a resistive load. The harvested power of the harvester is calculated as

$$P_p = \frac{V_p^2}{R_p}, \tag{15}$$

$$P_e = i_e^2 R_e, \tag{16}$$

where V_p is the total voltage on the piezoelectric bimorph beam, where the upper and lower layers are connected in series. This calculation is done from steady-state oscillations after the initial transient has died off. Since the primary goal of energy harvesters is to convert mechanical energy to electrical energy, this implies that this should be done in the most efficient way possible. Analytical prediction for optimal PE resistance load from impedance matching is

$$R_{p,\mathrm{opt,th}} = \frac{1}{\omega C_p}. \tag{17}$$

Here, ω is the angular frequency. The biggest efficiency of EM power generation occurs when the mechanical damping equals to the electrical one [34], that is $d_e = d_m$, which corresponds to the classical impedance-matching condition for vibration energy harvesters. Therefore, from Equations [10] and [11] and since $d_m = m\Omega_0/Q$, this condition becomes

$$\frac{(NBl)^2}{R_e + R_C} = \frac{m\Omega_0}{Q}, \tag{18}$$

with quality factor Q and oscillator natural frequency Ω_0. This can be manipulated to obtain

$$R_{e,\mathrm{opt,th}} = \frac{Q_m C_{\mathrm{EM}}^2}{m\Omega} + R_C = \frac{C_{\mathrm{EM}}^2}{d_m} + R_C. \tag{19}$$

5 | Sensitivity Analysis of Linear Hybrid Energy Harvesting System

Sensitivity analysis is employed to investigate how variations in input parameters influence the output of the model. By systematically perturbing each parameter, this method

quantifies the individual contributions of the parameters to the harvester output power. In general, it provides a framework for understanding how changes in system characteristics affect the performance and behavior of the energy harvesting device.

The nominal parameter values used in this study are summarized in Table 1. These values were selected based on the expected vibration frequencies during operation and by referencing previous work—specifically, the prototype hybrid harvester developed and tested in our laboratory, which has been the subject of earlier investigations [35, 36], see Figure 5—Reproduced with permission [36]. Copyright 2024, Engineering Mechanics.

TABLE 1 | Parameters for the analysis of the hybrid energy harvesting system.

Parameter	Symbol	Value	Unit
Mechanical			
Mass	m	92	g
Damping (mechanical)	d_m	0.326	Ns/m
Stiffness	k	1586	N/m
Piezoelectric			
PE coupling	θ	0.73	mN/V
PE load resistance	R_p	140	kΩ
Capacitance	C_p	52	nF
Electromagnetic			
EM coupling	C_{EM}	13.16	N/A
EM load resistance	R_e	1200	Ω
Coil resistance	R_C	152	Ω
Coil inductance	L_C	0.055	H
Excitation			
Excitation amplitude	$\ddot{z}$	1	m/s^2
Excitation frequency	f	20.9	Hz

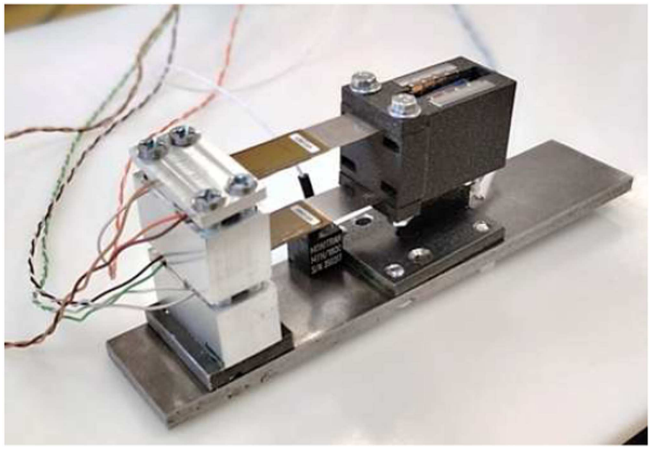

FIGURE 5 | The prototype hybrid PE-EM energy harvester, which was fabricated and experimentally validated. This prototype serves as a reference for selecting the nominal parameters employed in the present research. Reproduced with permission [36]. Copyright 2024, Engineering Mechanics.

5.1 | Local One-Factor-at-a-Time Sensitivity of Input Parameters

In order to gain intuition about the energy harvesting system and understand the system's sensitivity to key variables, the one-factor-at-a-time method was employed. The first simulation model described by Equations (1)–(3) is used for this preliminary analysis. In such a method, a total of N_p parameters are varied, where in each simulation, only one of the parameters is increased or decreased from its nominal value. This method provides a straightforward means of identifying which parameters have the most significant influence on system performance.

We test all $N_p = 12$ parameters of the hybrid PE–EM harvester, and a small change of 5% from the nominal values in both directions is assumed. We note that realistically, some parameters have much bigger uncertainties than others, but this will be dealt with later. In this section, we test the same uncertainty for all parameters and do not assume anything about the real distribution of the parameters. The idea here is just to test the upper and lower boundaries of each parameter and assume that the actual value for one harvester is somewhere in between.

Together with the simulation for nominal values, a total of $2N_p + 1$ simulations are performed. For each simulation, the transient behavior is discarded, and the values of average harvested power on load resistances for stationary behavior are recorded for both the piezoelectric and electromagnetic converters.

The results that can be seen separately for each converter in Figure 6 and for the total summed power in Figure 7 are not only quantitative but also qualitative. This means that they show not only if the generated power increases or decreases but also by how much it changes with a constant increase or a decrease in input values.

By comparing the collected data, the influence of variations in individual parameters on the system response can be clearly identified. The results clearly show that, by its physical nature, the resonance system exhibits the highest sensitivity to the excitation frequency and to parameters that effectively govern mass and stiffness. This implies that, in a population of nominally identical harvesters, even small deviations arising from manufacturing tolerances or mounting conditions may lead to noticeable shifts in the resonant frequency, potentially reducing the effectiveness of purely linear designs when operated under fixed-frequency excitation.

Importantly, the high sensitivity of these host-structure-related parameters motivates a different design philosophy. Instead of attempting to eliminate their uncertainty—which is unrealistic in industrial environments—their influence can be deliberately exploited for post-assembly fine-tuning of the harvester, for instance, through small adjustments of added mass or effective stiffness, in a manner analogous to mechanical balancing. From an industrial deployment perspective, such tuning should be regarded not as an optional refinement but as a mandatory step, precisely because these parameters are both highly sensitive and inherently uncertain.

On this basis, the subsequent analyses focus on energy-harvester-specific parameters that are more suitable for uncertainty-aware design and optimization across different

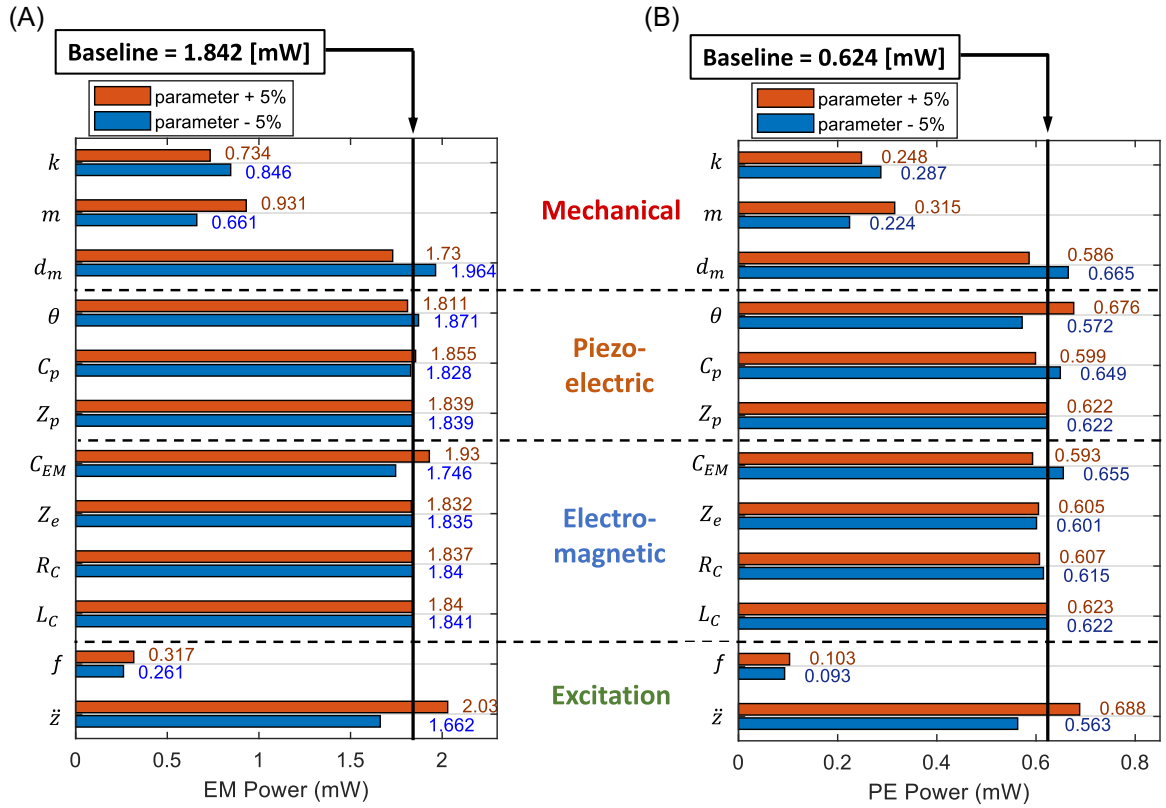

FIGURE 6 | Change in average generated power on load resistances with ***5***% change in the input parameters. Plot (A) shows the generated power on the electromagnetic converter, and plot (B) shows the generated power on the piezoelectric one. The blue lines indicate a decrease, and the red lines indicate an increase in the input parameter value. Nominal values that generated the baselines are indicated by black vertical lines. The parameters are divided into the four subsystems mentioned.

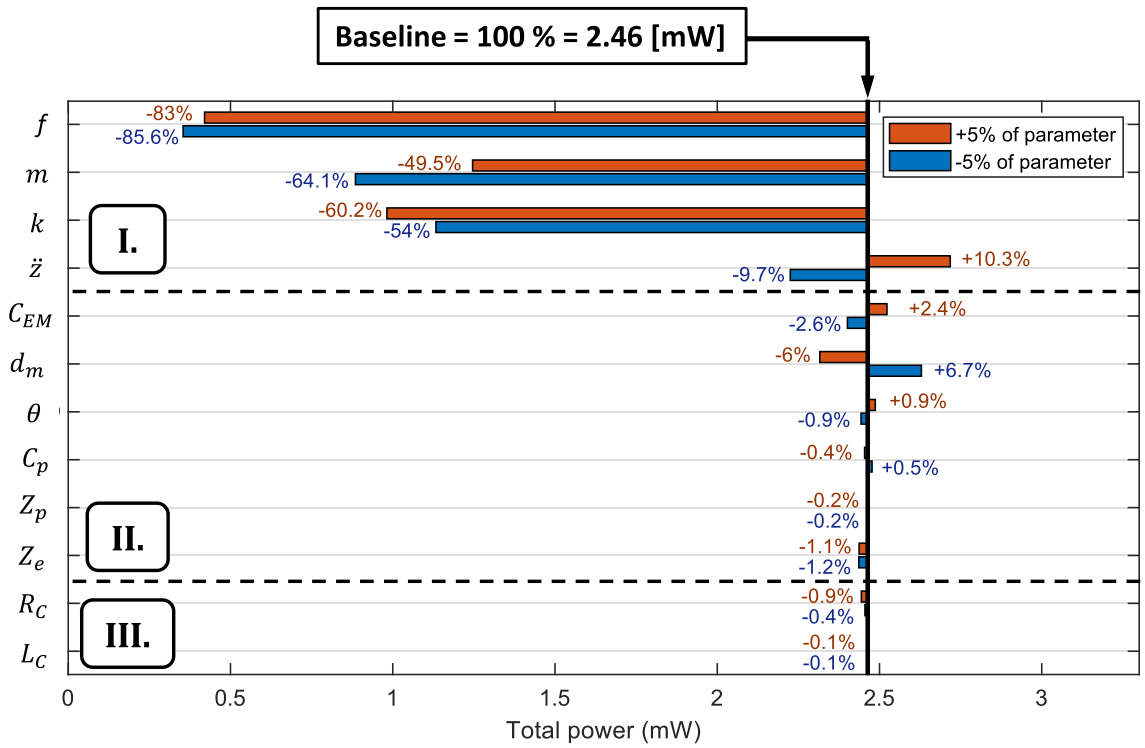

FIGURE 7 | Tornado sensitivity chart for average generated power when compared to the simulation with baseline values for all parameters. Area I. denotes tunable parameters. Area II. are parameters for possible further studies, and Area III. denotes negligible parameters.

applications. This observation is consistent with the extensive use of nonlinear strategies to broaden the effective resonance bandwidth. Several additional observations can be drawn from the results:

(1) More power is generated with smaller mechanical damping d_m, and

(2) with bigger excitation amplitude $\ddot{z}$.

(3) Coil inductance seems to be negligible to the system; therefore, it can be neglected and the term $L_C \frac{\mathrm{d}i_e}{\mathrm{d}t}$ is not considered in equations of motion.

(4) Since coil resistance is at least an order of magnitude smaller than load resistance for the EM converter, 5% uncertainty results only in $\pm 0.2\%$ change in the output and hence will remain in the equations of motion but can be neglected when it comes to sensitivity and uncertainty.

(5) Piezoelectric capacitance only affects the PE converter and not the EM one.

(6) Changes to both pure resistances R_p and R_e in both directions lead to a decrease in generated power, which means that they are at their optimum values. The impact of their uncertainty is minimal since the optimal resistance peak is quite shallow.

(7) The effects of PE and EM couplings are more complex and require further study; however, within the scope of the coupled 1DOF model, they provide a clear basis for evaluating the effectiveness of the individual converters as well as the potential benefits of employing both simultaneously.

6 | Global Sensitivity and Uncertainty Analysis

The local sensitivity analysis presented in Section 4 provided qualitative insight into the relative influence of individual parameters and enabled an initial screening of dominant effects. However, one-factor-at-a-time approaches cannot capture parameter interactions or quantify the combined impact of multiple simultaneous uncertainties.

To address these limitations, this section focuses on a global sensitivity and uncertainty analysis, in which all relevant uncertain parameters are varied simultaneously according to prescribed probability distributions. This approach enables a statistically consistent assessment of uncertainty propagation, interaction effects, and robustness of the hybrid energy harvester under realistic industrial conditions.

In contrast to the local sensitivity study, the uncertainties considered here are defined to reflect plausible manufacturing variability, material property scatter, and excitation uncertainty, thereby providing a more representative picture of expected performance variability in practice.

6.1 | Assessment of Possible Sources of Uncertainties

In industrial applications, energy harvesters are subject to a wide range of internal and external variability sources that can cause deviations of input parameters from their nominal values. These uncertainties originate from manufacturing tolerances, material property scatter, assembly imperfections, and variability of operational excitation.

To enable a structured and transparent uncertainty model, the dominant sources of variability considered in this study are summarized in Table 2. The listed sources do not represent an exhaustive set of all possible uncertainties, but rather a practically relevant subset that is expected to have the most significant influence on the performance of vibration-based hybrid energy harvesters.

Some factors have a bigger effect than others, and we also note that some parameters influence each other. Therefore, it is difficult to quantify the uncertainties precisely. We note that the

TABLE 2 | Overview of real-world sources of uncertainties for input parameters.

Parameter	Symbol	Source of uncertainty
Mechanical		
Damping	d_m	Material properties, clamping of the beam, vibration amplitude, and air resistance.
Excitation amplitude	$\ddot{z}$	Vibration shaker
Mode shape function	$\phi_{,x}(L_p)/\phi(L)$	FEM discretization
Electromagnetic		
Magnetic induction	B	B is spatially not constant, magnet properties, misalignment in magnet placement
Active coil length	Nl	Increase of coil diameter with more turns, coil holder manufacturing tolerances
Wire thickness	D	Manufacturing tolerances
Piezoelectric		
Permittivity	ε_{33}	Material properties of PZT
Stress-charge constant	e_{31}	Material properties of PZT, amount of PZT fibers in MFC
MFC width	B_p	Manufacturing tolerances
MFC length	L_p	Manufacturing tolerances, gluing misalignment
MFC thickness	t_p	Manufacturing tolerances, glue layer thickness
Substrate thickness	t_s	Manufacturing tolerances – sheet forming

used coil is thought to have $N = 900$ turns and an active length $l = 40$ mm per turn.

6.2 | Simulation Results for Global Sensitivity Analysis of Hybrid Kinetic Energy Harvester

The sensitivity analysis is performed using the Global Sensitivity and Uncertainty Analysis toolbox in the MATLAB environment. We define a vector of input parameter values, which are about to be varied together with their individual uncertainties, see Table 3. The assigned uncertainty levels represent a design-stage uncertainty model that combines both epistemic and aleatory sources of uncertainty. Epistemic uncertainty arises from limited knowledge of material properties, manufacturing variability, and assembly tolerances, while aleatory uncertainty reflects inherent variability observed in experimental measurements and operating conditions. Where available, prior experimental scatter, manufacturing tolerances, or measurement repeatability were used to define the standard deviations. For parameters for which detailed statistical data are not available at the current development stage, conservative design-stage uncertainty assumptions commonly adopted in energy harvesting and mechanical system modeling literature were applied.

Total generated power is the sum of powers from PE and EM converters and was chosen as the output variable.

The primary objective of this uncertainty analysis is not to predict exact production statistics, but to assess the relative robustness of the hybrid harvester design and to identify parameters whose variability most strongly affects output power. The classification in Table 3 explicitly distinguishes between uncertainties originating from experimental scatter, manufacturing tolerances, and design-stage assumptions, thereby improving transparency and reproducibility of the uncertainty model.

All input parameters are assumed to be normally distributed. Latin Hypercube sampling is used to generate a set of scenarios with different combinations of input values. These are then fed into a Simulink file containing the model described in Section 3. Latin Hypercube was chosen as the sampling method since it works with samples more efficiently than pure Monte Carlo methods. We run a total of 400 simulations for a time duration of $t = 5$ s. Figure 8 shows the histogram of the total generated power for the set of simulations.

TABLE 3 | Input normally distributed parameters for global uncertainty and sensitivity analysis.

Parameter	Symbol	Nominal value	Std. dev.	Std. dev %	Unit	Origin of uncertainty
Mechanical						
Damping	d_m	0.326	(0.065)	20%	Ns/m	Prior experimental scatter (free decay) [36]
Excitation amplitude	$\ddot{z}$	1	(0.01)	1%	m/s^2	Prior experimental scatter (measured vibration variability) [23]
Mode shape function	$\phi_x(L_p)/\phi(L)$	10.4	(1.04)	10%	m^{-2}	FEM approximation uncertainty [37]
Electromagnetic						
Magnetic induction	B	0.365	(0.0365)	10%	T	FEM approximation uncertainty [37]
Active coil length	Nl	36	(0.36)	1%	m	Manufacturing tolerances
Wire thickness	d	0.12	(0.0012)	1%	mm	Manufacturer tolerance [38]
Piezoelectric						
Permittivity	ε_{33}	2×10^{-8}	(1×10^{-9})	5%	F/m	Design-stage uncertainty assumption [39]
Stress-charge constant	e_{31}	8.32	(0.832)	10%	C/N	Design-stage uncertainty assumption [39] (MFC material variability)
MFC width	B_p	14	0.5	(3.5%)	mm	Manufacturing tolerance [40]
MFC length	L_p	28	2	(7%)	mm	Manufacturing tolerance [40] & bonding misalignment
MFC thickness	t_p	300	10	(3.3%)	μm	Manufacturing tolerance [40]
Substrate thickness	t_s	300	10	(3.3%)	μm	Manufacturing tolerance [41] + measurement uncertainty [18]
Output						
Total power	P	***2.47***	0.19	(7.5%)	mW	
Power on PE	P_p	***0.61***	0.10	(16.4%)	mW	
Power on EM	P_e	***1.85***	0.18	(9.7%)	mW	

Chi-squared goodness of fit on the 5% significance level did not reject the hypothesis that the output data for all three results (PE, EM, and total power) come from a normal distribution, indicating that the output power can be thought to behave normally. The variance in output power is approximately 7.5% of the nominal value.

Saltelli method was chosen for global sensitivity analysis because it provides a comprehensive assessment of the sensitivity of the output power to the inputs while considering their interactions. Also, sensitivity indices of any order can be calculated. Contrary to one-factor-at-a-time methods, the Saltelli method also enables us to calculate not only first-order sensitivity indices, but also total sensitivity indices.

Figure 9 shows total sensitivity indices, which are a measure of the influence of input parameters on the output. It can be seen that mechanical damping has the biggest effect. Input PE parameters influence mostly (but not entirely) the power generated on its corresponding transducer, and the same is true for the EM one. Magnetic induction B, as the only magnetic parameter, dominates over the design coil parameters (N, l) when it comes to coil design. Further optimization of the magnetic field is desirable. Therefore, caution must be taken when designing multiple harvesters, since possible inhomogeneities in the magnetic field and possibly also the variations in magnetic properties of the used magnets influence the generated power quite substantially.

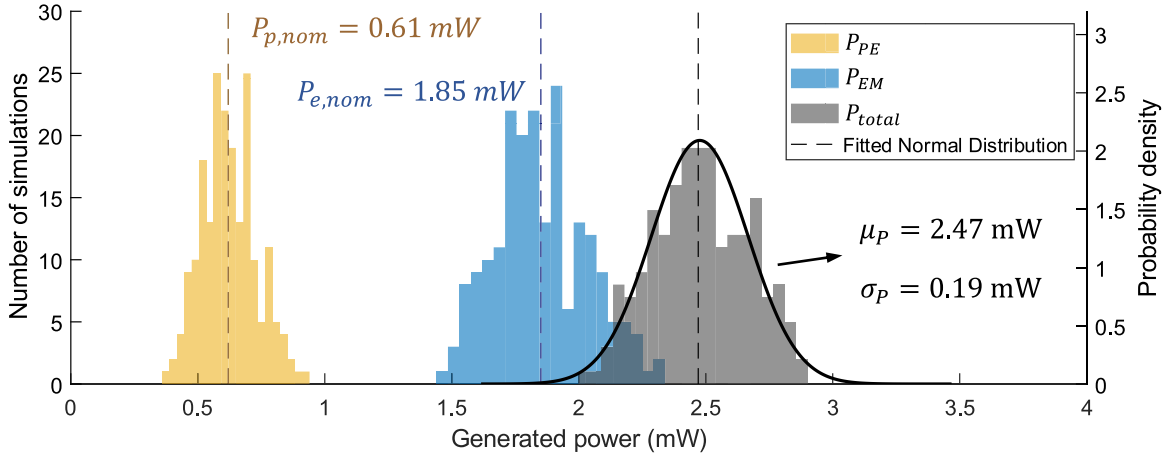

FIGURE 8 | Histogram of average generated power for all 400 simulations. The generated power on the PE transducer is orange, the power on the EM is blue, and their sum is in gray. The power that was generated for nominal values is shown by dashed lines. The thick black line shows the fitted normal distribution for total power.

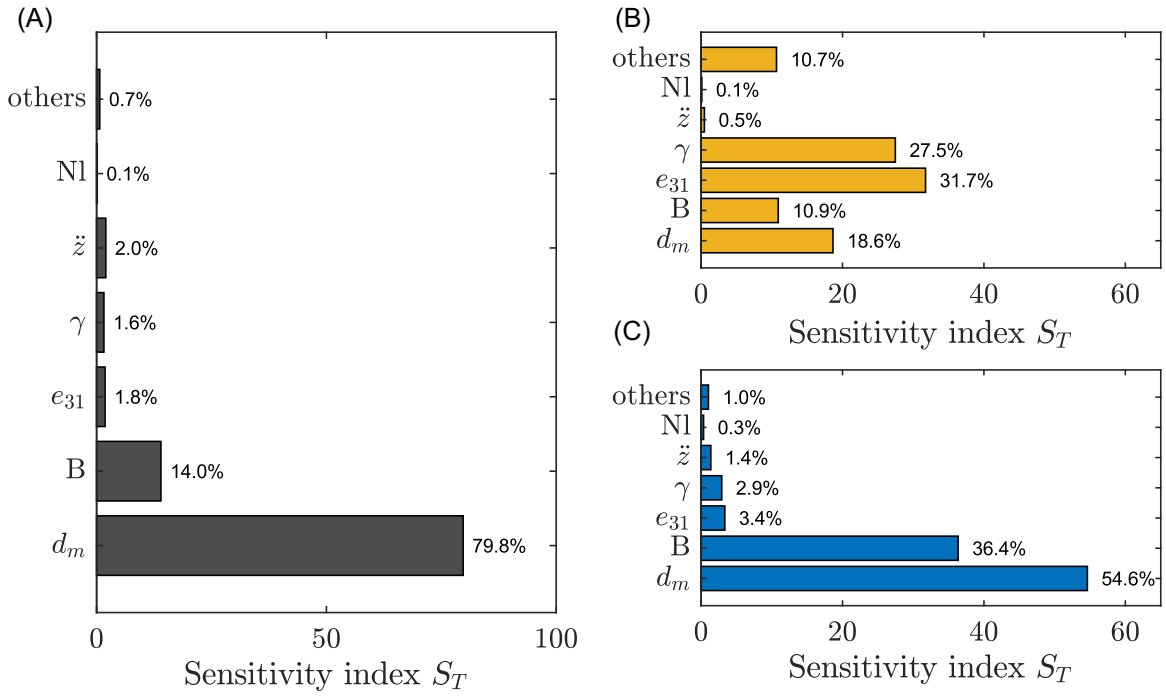

FIGURE 9 | Total sensitivity indices $\boldsymbol{S_T}$ for total generated power (A) and for power generated on the PE (B) and EM (C) resistive loads.

The mode shape, represented by the factor γ, clearly has a big effect on PE power since it relates to the bending of the PE layer but has a negligible effect on EM power. The same is true for the geometrical dimensions of the composite beam, mainly the thickness and length of the PE layer. Figure 9b puts them all as "others," but their sensitivity indices read $S_{L_p} = 3.3\%$, $S_{t_s} = 0.8\%$, $S_{t_p} = 3.6\%$, $S_{B_p} = 0.9\%$.

7 | Influence of Piezoelectric and Electromagnetic Couplings on Harvester Performance Under Real Vibrations

In this section, we take a deeper look at the effects of piezoelectric and electromagnetic couplings on the power output performance of the hybrid energy harvester. Equation (5) indicates that the generated power on the PE converter is mostly affected by the used material (its piezoelectric constant). Generally, for a standalone piezoelectric harvester, higher values of θ yield more power, but only until a critical value $\theta = \theta_{\text{crit}}$ is reached. Analytical predictions for this critical value have been developed and can be found, for example, in a paper by Daqaq [34]. It reads as follows:

$$\theta_{\text{crit}} = \sqrt{(4\zeta + 4\zeta^2)C_p k} \tag{20}$$

with mechanical damping ratio ζ, PE capacitance C_p, and stiffness k. For the parameters of this paper (see Table 1), this results in $\theta_{\text{crit}} = 2.1$ mN/V.

A corresponding critical value can also be derived for the electromagnetic harvester—the critical EM coupling $C_{\text{EM,crit}}$. This value can be easily derived from Equations (10) and (18). These equations are manipulated to obtain the formula for critical EM coupling as

$$C_{\text{EM,crit}} = \sqrt{(R_e + R_C)d_m} \tag{21}$$

which results in $C_{\text{EM,crit}} = 21$ N/A.

To assess the performance of the hybrid energy harvester under realistic industrial excitation, a representative example of measured vibration input was selected. Based on practical experience with vibration energy harvesting systems in transportation and industrial applications [3, 42, 43]—such as railways and aeronautics—these environments are typically characterized by broadband, noisy, and nonstationary vibrations with several dominant frequencies rather than idealized harmonic excitation.

Figure 10 shows a typical example of measured acceleration data representative of such industrial conditions, which is used here to evaluate the performance of the analyzed hybrid vibration energy harvester under realistic operating excitation.

The difference between the average power obtained under harmonic excitation (Figure 8) and under measured vibration input (Figure 10) is primarily attributed to differences in the excitation characteristics. The harmonic simulations are performed at a fixed excitation amplitude and at resonance, representing an idealized operating condition. In contrast, the measured acceleration signal exhibits a lower effective RMS amplitude and contains broadband, non-stationary frequency components.

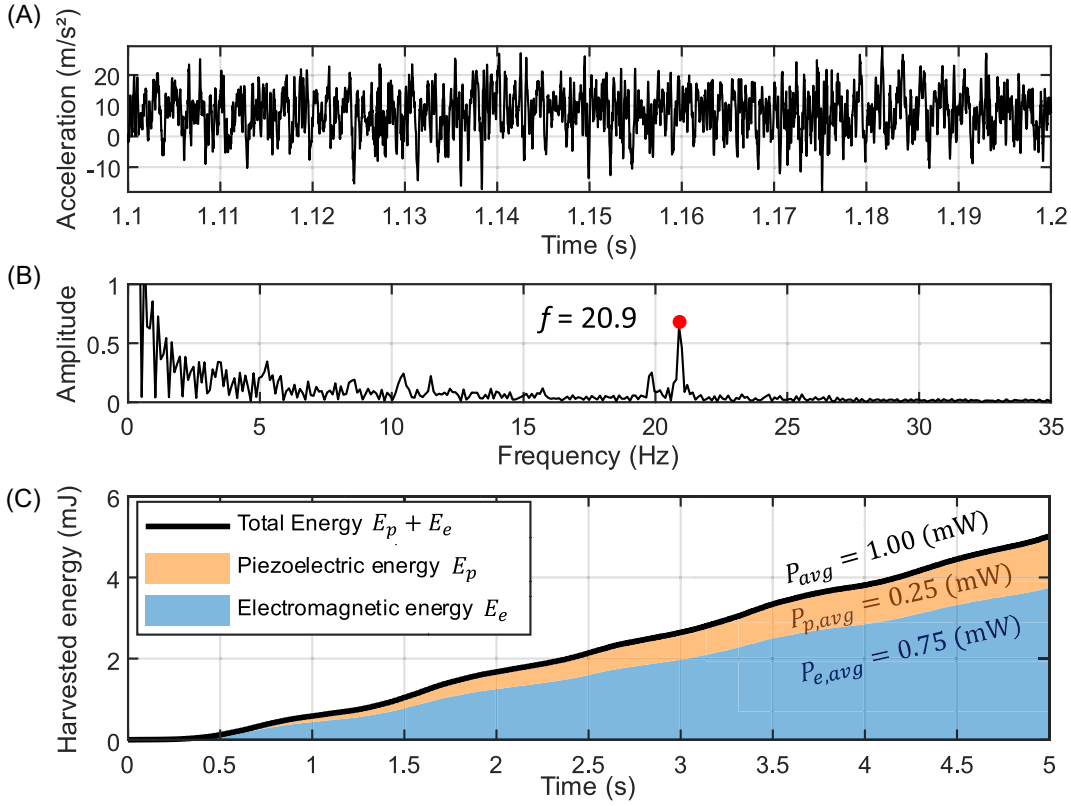

FIGURE 10 | Performance of the given hybrid energy harvester under real excitation. Plots (A) and (B) show the input measured acceleration data in time and frequency domains, respectively. Plot (C) shows generated energy and average power.

As a result, the harvester operates only intermittently close to its resonance frequency, leading to a reduced average power output. This behavior is consistent with expectations and highlights the importance of evaluating energy harvesters under realistic excitation conditions rather than relying solely on idealized harmonic inputs.

While this setup shows electric energy can be currently generated, the next step is to explore possible improvements. We simulated the system described by Equations (1)–(3) across a range of PE and EM coupling coefficients to investigate the effect of couplings on output power, namely:

- How the values of critical PE and EM couplings change for the hybrid harvester.
- Whether the current coupling values could be optimized.
- Whether such optimization would be practically beneficial.

The recorded total harvested power across a matrix of input coupling values θ and C_{EM} was done for many simulation results. The simulation results with an emphasis on the simulation of weak and strong electromechanical couplings of both converters are presented in Figure 11.

The results reveal a clearly non-monotonic dependence of total harvested power on both coupling coefficients. Increasing either piezoelectric or electromagnetic coupling improves power output only up to a certain level. Beyond this region, further coupling enhancement leads to excessive electrical damping, reduced mechanical vibration amplitudes, and consequently lower harvested power.

In the parameter space depicted in Figure 11, the coupling coefficients are treated as freely adjustable, although in practice, they are constrained by physical limitations. Point (1) is the current state, (2), (3), and (4) are points for possible improvement, (5) is the global maximum, point (6) corresponds to critical PE coupling, and critical EM coupling is at point (4). Figure 12 illustrates system behavior across various configurations with different coupling values.

These observations are consistent with previously reported findings [16, 17], which showed that hybrid piezoelectric–electromagnetic energy harvesters are advantageous only within intermediate coupling regimes, while both weak and overly strong coupling result in inferior performance. In particular, hybridization becomes beneficial only when neither transduction mechanism dominates the system dynamics and when electrical and mechanical damping contributions remain balanced.

Enhancing the PE coupling, for example, would require advanced materials with higher piezoelectric constants—an option that is often difficult to implement. Similarly, further increasing the EM coupling beyond its critical threshold brings no additional benefits as the system already exhibits strong electromagnetic interaction.

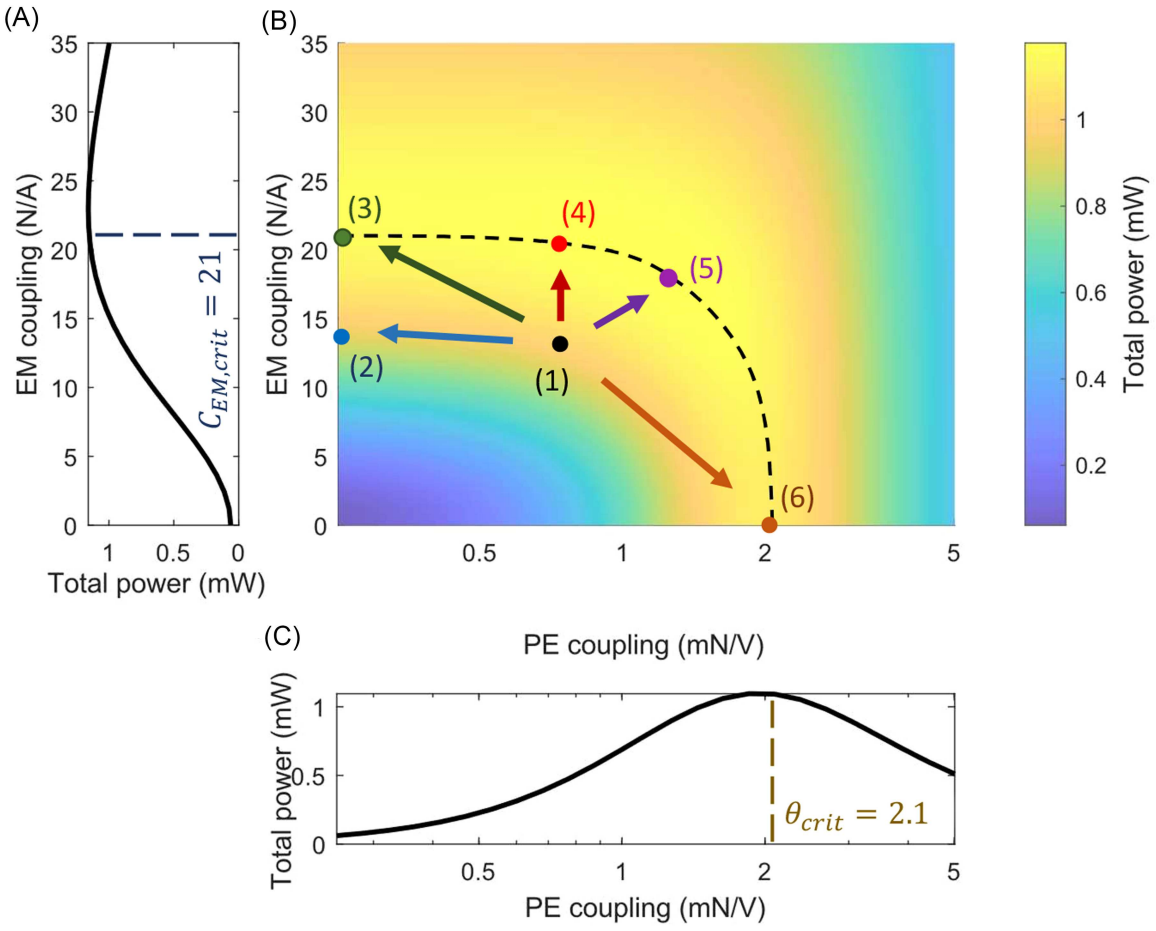

FIGURE 11 | Effect of piezoelectric and electromagnetic couplings on total generated power (B). Plot (A) is a section of the figure for $\theta = 0$, (pure EM harvester), and plot (C) is a section for $C_{\mathrm{EM}} = 0$, (for pure PE harvester).

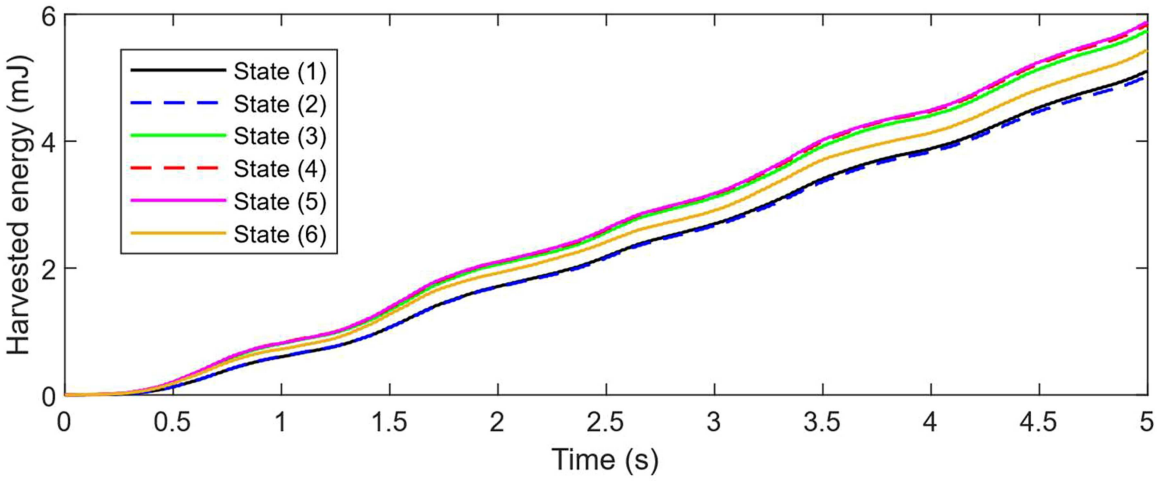

FIGURE 12 | Examples of harvested energy plots of possible hybrid energy harvesters with different coupling values.

TABLE 4 | Comparison of relevant parameters for the current state (1) and suggested points for improvement.

	Symbol	Unit	(1)	(2)	(3)	(4)	(5)	(6)
EM coupling	C_{EM}	N/A	13.15	16.6	21	20.4	18.1	0
PE coupling	θ	mN/V	0.73	0	0	0.73	1.81	2.0
EM power	P_e	mW	0.77	1.00	1.14	1.02	0.76	0
EM voltage	V_e	V	1.72	1.95	2.12	2.01	1.75	0
PE power	P_p	mW	0.24	0	0	0.14	0.41	1.08
PE voltage	V_p	V	10.77	0	0	8.32	14.26	23.5
Total power	$\boldsymbol{P}$	**mW**	**1.01**	**1.00**	**1.14**	**1.16**	**1.17**	**1.08**

Although the global maximum (5) is unreachable in practice, feasible optimization strategies therefore focus primarily on the electromagnetic subsystem. For example, point (2) represents a pure EM generator matching the power of the current hybrid state (point 1) with only a slight increase in EM coupling, $C_{\mathrm{EM},6} = 15.6$ (corresponding coil parameters in Table 4).

Therefore, all feasible improvement strategies involve increasing EM coupling. This could be achieved by using larger or stronger magnets or increasing the coil size. However, such modifications would most likely influence system mass, damping, and other crucial factors. A more refined approach is to increase the number of coil turns and operation of optimal resistive load while reducing wire diameter—though this increases the coil's electrical resistance and must be approached carefully.

Overall, Figure 11 can be interpreted as a design map rather than a single-device optimization result. If the achievable coupling parameters lie close to the boundaries of the parameter space, a pure EM or pure PE harvester is preferable. Hybrid configurations become advantageous only in the intermediate coupling region, where balanced electromechanical interaction enables improved energy conversion efficiency.

8 | Conclusion

This paper investigated uncertainty, sensitivity, and efficiency aspects of a hybrid piezoelectric–electromagnetic vibration energy harvester with the aim of supporting reliable industrial deployment. Beyond individual analyses reported in prior works, the study was conceived as a comprehensive investigation that brings together local sensitivity analysis, global uncertainty quantification, and efficiency assessment within a single, coherent framework. The traditional 1-degree-of-freedom model of a hybrid energy harvester was enhanced by including realistic design variables, such as geometry tolerances and material properties variation. This enabled a deeper and more systematic analysis than is typically presented and makes the results directly relevant for industrial-scale deployment.

Our analysis shows how different system parameters influence the amount of power the harvester can generate. Using tornado charts and sensitivity indices, we highlighted which parameters matter the most. These visual tools offer a simple way to understand the relative importance of each factor and help guide smarter design decisions.

We also considered manufacturing and industrial uncertainties and quantified how much they can affect the output power. By including these uncertainties in a global sensitivity analysis (Saltelli method), we were able to predict the expected range of output power for both the piezoelectric and electromagnetic parts of the system. This gave us a clearer view of the variability expected in industrial production scenarios.

In addition, we examined how well the piezoelectric and electromagnetic subsystems work together. We found that

piezoelectric coupling plays a smaller role than electromagnetic effects and often introduces extra mechanical damping, which can reduce performance. The figures included in this paper can help engineers and designers decide whether combining both technologies (hybridization) makes sense for their application. In many cases, a kinetic electromagnetic harvester alone is the better choice. Adding a piezoelectric converter can sometimes make the system more complex without improving performance. Piezoelectric patches with stronger coupling factors provide higher mechanical damping of resonators, which significantly decreases maximal electrical power. Still, there are situations where either a pure piezoelectric harvester setup can be beneficial, depending on the vibration source and system constraints, e.g., miniaturization of the harvesting system.

A hybrid system is used in this analysis to make the comparison and evaluation comprehensible for both electromagnetic and piezoelectric approaches, and the results are transferable to pure electromagnetic or piezoelectric converters. However, based on the results, in the case of the hybrid harvester, it is more effective to maximize the performance of either the electromagnetic or piezoelectric component individually. This insight is a key contribution of the paper.

The results of this comprehensive study demonstrate that the governing parameters of vibration energy harvesters can be systematically divided into two fundamentally different groups within a unified analysis framework. Primarily, parameters determining the resonance condition—most notably effective stiffness and mass—exhibit extremely high sensitivity. Because uncertainties cannot be eliminated in industrial practice, precise post-assembly tuning to achieve resonance is mandatory. Rather than attempting to suppress these uncertainties, robust deployment requires adapting the harvester to actual operating conditions. Second, the remaining parameters associated with piezoelectric and electromagnetic transduction and electrical loading exhibit more structured and manageable sensitivities, making them well-suited for systematic sensitivity ranking and uncertainty-aware analysis within the comprehensive framework proposed in this work.

Overall, this study provides useful and practical guidance for designing more efficient and reliable kinetic energy harvesters. While our focus was on one specific device, the proposed comprehensive framework for sensitivity and uncertainty analysis is general and can be applied to a broad class of vibration energy harvesting systems. Future research should explore nonlinearities, particularly magnetic interactions, and pursue global optimization of system parameters to refine design strategies and enhance performance.

Acknowledgments

This publication was supported by the project "Mechanical Engineering of Biological and Bio-inspired Systems," funded as project No. CZ.02.01.01/00/22_008/0004634 by Program Johannes Amos Commenius, call Excellent Research. Additionally, authors gratefully acknowledge support provided by the project GAČR no. 25-14505L Advanced techniques for effective kinetic nonlinear energy harvesting technologies.

Conflicts of Interest

The authors declare no conflicts of interest.

Data Availability Statement

The data that support the findings of this study are openly available in Zenodo at https://zenodo.org/uploads/10794063, reference number 10.5281/zenodo.10794063.

References

1. C. Wei and X. Jing, "A Comprehensive Review on Vibration Energy Harvesting: Modelling and Realization," *Renewable and Sustainable Energy Reviews* 74 (2017): 1–18, https://doi.org/10.1016/J.RSER.2017.01.073.

2. O. Kanoun, ed., "Energy Wireless Sensor Networks: Technology, Components and System Design," in *Energy Harvesting for Wireless Sensor Networks: Technology, Components and System Design* (De Gruyter Oldenbourg, 2018), 1–386, https://doi.org/10.1515/9783110445053.

3. Z. Hadas, O. Rubes, F. Ksica, and J. Chalupa, "Kinetic Electromagnetic Energy Harvester for Railway Applications—Development and Test With Wireless Sensor," *Sensors* 22, no. 3 (2022): 905, https://doi.org/10.3390/S22030905.

4. M. A. Bănică, "Energy Harvesting from Renewable Energy Sources." *Lecture Notes in Networks and Systems*, Vol. 85 (Springer, 2020), 247–254. https://doi.org/10.1007/978-3-030-26991-3_23.

5. D. K. Sah and T. Amgoth, "Renewable Energy Harvesting Schemes in Wireless Sensor Networks: A Survey," *Information Fusion* 63 (2020): 223–247, https://doi.org/10.1016/j.inffus.2020.07.005.

6. M. A. Abdelnaby, M. S. Shiba, and S. Ali, "Numerical Investigations of Bistable Piezoelectric Cantilever for Enhanced Energy Harvesting," *IOP Conference Series: Materials Science and Engineering* 973, no. 1 (2020): 012022, https://doi.org/10.1088/1757-899X/973/1/012022.

7. M. Płaczek, "Modelling and Production Process of the Energy Harvesting System Based on Mfc Piezoelectric Transducers," *International Journal of Modern Manufacturing Technologies* 12, no. 3 (2020): 106–114.

8. Z. Li, Y. Liu, P. Yin, et al., "Constituting Abrupt Magnetic Flux Density Change for Power Density Improvement in Electromagnetic Energy Harvesting," *International Journal of Mechanical Sciences* 198 (2021): 106363, https://doi.org/10.1016/J.IJMECSCI.2021.106363.

9. J. Xing, S. Fang, X. Fu, and W. H. Liao, "A Rotational Hybrid Energy Harvester Utilizing Bistability for Low-Frequency Applications: Modelling and Experimental Validation," *International Journal of Mechanical Sciences* 222 (2022): 107235, https://doi.org/10.1016/J.IJMECSCI.2022.107235.

10. J. Margielewicz, D. Gąska, G. Litak, P. Wolszczak, and D. Yurchenko, "Influence of Impulse Characteristics on Realizing High-Energy Orbits in Hybrid Energy Harvester," *Energy Conversion and Management* 277 (2023): 116672, https://doi.org/10.1016/J.ENCONMAN.2023.116672.

11. T. Yang and Q. Cao, "Dynamics and Energy Generation of a Hybrid Energy Harvester Under Colored Noise Excitations," *Mechanical Systems and Signal Processing* 121 (2019): 745–766, https://doi.org/10.1016/j.ymssp.2018.12.004.

12. B. Yang, "Hybrid Energy Harvester Based on Piezoelectric and Electromagnetic Mechanisms," *Journal of Micro/Nanolithography, MEMS, and MOEMS* 9, no. 2 (2010): 023002, https://doi.org/10.1117/1.3373516.

13. K. Niazi, M. J. K. Parsi, and M. Mohammadi, "Nonlinear Dynamic Analysis of Hybrid Piezoelectric-Magnetostrictive Energy-Harvesting Systems," *Journal of Sensors* 2022 (2022): 1–23, https://doi.org/10.1155/2022/8921779.

14. H. Ryu, H. J. Yoon, and S. W. Kim, "Hybrid Energy Harvesters: Toward Sustainable Energy Harvesting," *Advanced Materials* 31, no. 34 (2019): 1802898, https://doi.org/10.1002/adma.201802898.

15. A. Othman, J. Hrad, J. Hajek, and D. Maga, "Control Strategies of Hybrid Energy Harvesting—A Survey," *Sustainability* 14, no. 24 (2022): 16670, https://doi.org/10.3390/su142416670.

16. B. D. Truong, C. P. Le, and S. Roundy, "Are Piezoelectric-Electromagnetic Hybrid Energy Harvesting Systems Beneficial?," *Smart Materials and Structures* 32, no. 9 (2023): 095022, https://doi.org/10.1088/1361-665X/ACEC23.

17. I. Bahadur, H. Ouakad, E. M. Barhoumi, et al., "Performance Comparison of Hybrid and Standalone Piezoelectric Energy Harvesters Under Vortex-Induced Vibrations," *Modelling* 6, no. 4 (2025): 120, https://doi.org/10.3390/MODELLING6040120.

18. P. Peralta, R. O. Ruiz, and V. Meruane, "Experimental Study of the Variations in the Electromechanical Properties of Piezoelectric Energy Harvesters and Their Impact on the Frequency Response Function," *Mechanical Systems and Signal Processing* 115 (2019): 469–482, https://doi.org/10.1016/J.YMSSP.2018.06.002.

19. R. Madankan, M. A. Karami, and P. Singla, "Uncertainty Analysis of Energy Harvesting Systems," *Proceedings of the ASME Design Engineering Technical Conference* 6 (2014): 6, https://doi.org/10.1115/DETC201435480.

20. B. P. Mann, D. A. Barton, and B. A. Owens, "Uncertainty in Performance for Linear and Nonlinear Energy Harvesting Strategies," *Journal of Intelligent Material Systems and Structures* 23, no. 13 (2012): 1451–1460, https://doi.org/10.1177/1045389X12439639.

21. R. Aloui, W. Larbi, and M. Chouchane, "Uncertainty Quantification and Global Sensitivity Analysis of Piezoelectric Energy Harvesting Using Macro Fiber Composites," *Smart Materials and Structures* 29, no. 9 (2020): 095014. https://doi.org/10.1088/1361-665X/ab9f12.

22. P. Sosna and Z. Hadaš, "Influence of Geometric and Material Uncertainties on the Behavior of Monostable and Bistable Electromagnetic Energy Harvesters," *Sensors* 26, no. 1 (2025): 253, https://doi.org/10.3390/S26010253.

23. J. P. Norenberg, A. Cunha, S. da Silva, and P. S. Varoto, "Global Sensitivity Analysis of Asymmetric Energy Harvesters," *Nonlinear Dynamics* 109, no. 2 (2022): 443–458, https://doi.org/10.1007/S11071-022-07563-8.

24. Y. Li, S. Zhou, and G. Litak, "Uncertainty Analysis of Bistable Vibration Energy Harvesters Based on the Improved Interval Extension," *Journal of Vibration Engineering & Technologies* 8, no. 2 (2020): 297–306, https://doi.org/10.1007/s42417-019-00134-z.

25. P. H. Martins and A. A. Santos, "Metamodeling for Robust Design of Energy Harvesting Devices Using Multiobjective Optimizations," *International Journal of Mechanics and Materials in Design* 21, no. 6 (2025): 1857–1877, https://doi.org/10.1007/S10999-025-09804-1.

26. M. Rajarathinam and S. F. Ali, "Parametric Uncertainty and Random Excitation in Energy Harvesting Dynamic Vibration Absorber," *ASCE-ASME Journal of Risk and Uncertainty in Engineering Systems, Part B: Mechanical Engineering* 7, no. 1 (2021): 010905, https://doi.org/10.1115/1.4049211.

27. H. Uluşan, S. Chamanian, W. M. P. R. Pathirana, Zorlu, A. Muhtaroğlu, and H. Külah, "Triple Hybrid Energy Harvesting Interface Electronics," *Journal of Physics: Conference Series* 773, no. 1 (2016): 012027, https://doi.org/10.1088/1742-6596/773/1/012027.

28. W. Qing-Ming wang and L. E. Cross, "Constitutive Equations of Symmetrical Triple Layer Piezoelectric Benders," *IEEE Transactions on Ultrasonics, Ferroelectrics, and Frequency Control* 46, no. 6 (1999): 1343–1351, https://doi.org/10.1109/58.808857.

29. S. C. Stanton, C. C. McGehee, and B. P. Mann, "Nonlinear Dynamics for Broadband Energy Harvesting: Investigation of a Bistable Piezoelectric Inertial Generator," *Physica D: Nonlinear Phenomena* 239, no. 10 (2010): 640–653, https://doi.org/10.1016/j.physd.2010.01.019.

30. T. Daue and J. Kunzmann, "Energy Harvesting Systems Using Piezo-Electric MFCs," in *2008 17th IEEE International Symposium on the Applications of Ferroelectrics, Santa Re, NM, USA* (2008), 1, https://doi.org/10.1109/ISAF.2008.4693937.

31. A. Mystkowski and V. Ostasevicius, "Experimental Study of Macro Fiber Composite-Magnet Energy Harvester for Self-Powered Active Magnetic Bearing Rotor Vibration Sensor," *Energies* 13 (2020): 4806, https://doi.org/10.3390/en13184806.

32. Z. Hadas, F. Ksica, and O. Rubes, "Piezoceramic Patches for Energy Harvesting and Sensing Purposes," *European Physical Journal Special Topics* 228 no. 7 (2019): 1589–1604, https://doi.org/10.1140/EPJST/E2019-800156-6.

33. R. Gherca and R. Olaru, "Power Analysis for an Electromagnetic Generator With Magnets Destined to Vibration Energy Harvesting," in *EPE 2012 - Proceedings of the 2012 International Conference and Exposition on Electrical and Power Engineering* (IEEE, 2012), 485–490, https://doi.org/10.1109/ICEPE.2012.6463886.

34. J. M. Renno, M. F. Daqaq, and D. J. Inman, "On the Optimal Energy Harvesting From a Vibration Source," *Journal of Sound and Vibration* 320, no. 1/2 (2009): 386–405, https://doi.org/10.1016/j.jsv.2008.07.029.

35. P. Sosna and Z. Hadas, "Power Optimization of Hybrid Energy Harvestering From Mechanical Vibrations Using Piezoelectric and Electromagnetic Mechanisms,"in *Proceedings of the 2024 21st International Conference on Mechatronics - Mechatronika, ME* (IEEE, 2024), https://doi.org/10.1109/ME61309.2024.10789724.

36. P. Sosna and Z. Hadaš, "Development and Verification of Novel Dual Plunger Hybrid Kinetic Energy Harvester," in *Engineering Mechanics* (2024), 286–289, https://doi.org/10.21495/EM2024-286.

37. D. Meeker, Finite Element Method Magnetics User's Manual, Version 4.2 (2015), http://www.femm.info/wiki/HomePage.

38. International Electrotechnical Commission, *IEC 60317-0-1: Specifications for Particular Types of Winding Wires* (International Electrotechnical Commission, 2013).

39. Y. Xiao and N. Wu, "Uncertainty Analysis of Nonlinear Piezoelectric Energy Generator Under Friction," in *Lecture Notes in Mechanical Engineering* (2025), 75–86, https://doi.org/10.1007/978-981-96-1191-1_7.

40. Smart Material Corporation, *Macro Fiber Composite (MFC) Datasheet (M-2814-P2)* (2019), https://smart-material.com/.

41. European Committee for Standardization, EN 10131: Cold Rolled Uncoated Steel Flat Products – Tolerances on Dimensions and Shape (CEN, 2016).

42. S. Zelenika, Z. Hadas, S. Bader, et al., "Energy Harvesting Technologies for Structural Health Monitoring of Airplane Components—A Review," *Sensors* 20, no. 22 (2020): 6685, https://doi.org/10.3390/s20226685.

43. O. Rubes, J. Chalupa, F. Ksica, and Z. Hadas, "Development and Experimental Validation of Self-Powered Wireless Vibration Sensor Node Using Vibration Energy Harvester," *Mechanical Systems and Signal Processing* 160 (2021): 107890, https://doi.org/10.1016/j.ymssp.2021.107890.